Inflammation Research (2022) 71:131–140
https://doi.org/10.1007/s00011-021-01525-3

Inflammation Research

ORIGINAL RESEARCH ARTICLE

Severity of SARS-CoV-2 infection is linked to double-negative ($CD27^-$ IgD^-) B cell subset numbers

Rodrigo Cervantes-Díaz[1,2] · Víctor Andrés Sosa-Hernández[1,3] · Jiram Torres-Ruíz[4,5] · Sandra Romero-Ramírez[1,2] · Mariana Cañez-Hernández[1] · Alfredo Pérez-Fragoso[4] · José C. Páez-Franco[1] · David E. Meza-Sánchez[1] · Miriam Pescador-Rojas[6] · Víctor Adrián Sosa-Hernández[7] · Diana Gómez-Martín[4] · José L. Maravillas-Montero[1]

Received: 8 June 2021 / Revised: 1 October 2021 / Accepted: 2 November 2021 / Published online: 30 November 2021

Abstract

Objectives The role of B cells in COVID-19, beyond the production of specific antibodies against SARS-CoV-2, is still not well understood. Here, we describe the novel landscape of circulating double-negative (DN) $CD27^-$ IgD^- B cells in COVID-19 patients, representing a group of atypical and neglected subpopulations of this cell lineage.

Methods Using multiparametric flow cytometry, we determined DN B cell subset amounts from 91 COVID-19 patients, correlated those with cytokines, clinical and laboratory parameters, and segregated them by principal components analysis.

Results We detected significant increments in the DN2 and DN3 B cell subsets, while we found a relevant decrease in the DN1 B cell subpopulation, according to disease severity and patient outcomes. These DN cell numbers also appeared to correlate with pro- or anti-inflammatory signatures, respectively, and contributed to the segregation of the patients into disease severity groups.

Conclusion This study provides insights into DN B cell subsets' potential role in immune responses against SARS-CoV-2, particularly linked to the severity of COVID-19.

Keywords B cell · DN B cell · COVID-19 · Inflammation

Abbreviations

ALT	Alanine aminotransferase
Alb	Albumin
ASC	Antibody-secreting cells
AST	Aspartate aminotransferase
BCR	B cell receptor
Breg	Regulatory B cells
COVID-19	Coronavirus disease 2019
CRP	C-reactive protein
DaSO	Days after symptom onset
Dd	D-dimer
DN	Double-negative B cells
Fib	Fibrinogen
FMO	Fluorescence minus one
HIV	Human immunodeficiency viruses
IP-10/CXCL10	Interferon gamma-induced protein
LDH	Lactate dehydrogenase
Lk	Leukocyte

Responsible Editor: Anatoliy Kubyshkin.

Rodrigo Cervantes-Díaz and Víctor Andrés Sosa-Hernández contributed equally to this work.

✉ José L. Maravillas-Montero
maravillas@cic.unam.mx

[1] Red de Apoyo a la Investigación, Universidad Nacional Autónoma de México e Instituto Nacional de Ciencias Médicas y Nutrición Salvador Zubirán, Mexico City, Mexico

[2] Facultad de Medicina, Universidad Nacional Autónoma de México, Mexico City, Mexico

[3] Departamento de Biomedicina Molecular, Centro de Investigación y de Estudios Avanzados del Instituto Politécnico Nacional, Mexico City, Mexico

[4] Departamento de Inmunología y Reumatología, Instituto Nacional de Ciencias Médicas y Nutrición Salvador Zubirán, Mexico City, Mexico

[5] Departamento de Atención Institucional Continua y Urgencias, Instituto Nacional de Ciencias Médicas y Nutrición Salvador Zubirán, Mexico City, Mexico

[6] Escuela Superior de Cómputo, Instituto Politécnico Nacional, Mexico City, Mexico

[7] School of Engineering and Science, Tecnológico de Monterrey, Mexico, Mexico

Lt	Lymphocyte
MCP-1/CCL2	Monocyte chemoattractant protein 1
Nt	Neutrophil
PaO_2/FiO_2 or PaFi	Arterial partial pressure of oxygen (PaO_2)/Fraction of inspired oxygen (FiO_2) ratio
PBMCs	Peripheral blood mononuclear cells
PCA	Principal component analysis
RR	Respiratory rate
SARS-CoV-2	Severe acute respiratory syndrome coronavirus 2
SLE	Systemic lupus erythematosus
SO_2	Oxygen saturation
SwM	Switched-memory B cells
T1/T2	Transitional B cells
TLRs	Toll-like receptors
Treg	Regulatory T cells
Trp	Troponin
USwM	Unswitched-memory B cells

Introduction

B cells represent one of the main elements of the adaptive humoral immune system since they are responsible for mediating the production of antibodies directed against potential pathogens. The canonical classification strategies segregate human circulating B cells into different populations: transitional B cells ($CD24^{hi}$ $CD38^{hi}$ $CD27^{-}$) that constitutes recent bone marrow emigrants, naïve B cells ($CD38^{lo/-}$ $CD27^{-}$ IgD^{+}) representing mature B cells that have never been stimulated by their cognate antigens, memory B cells ($CD38^{lo/-}$ $CD27^{+}$) that are developed following a primary infection and remain in a quiescent state until they encounter the same antigen to become activated and induce a robust secondary response that includes their differentiation into plasmablasts/plasma cells ($CD38^{hi}$ $CD27^{hi}$) which are the responsible for antibody secretion [1].

Recently, the development of single-cell genomic approaches and high-dimensional flow cytometry has allowed identifying emerging B cell populations with distinctive phenotypes and divergent functional characteristics [2, 3]. In 2007, it was described the expansion of an unknown B cell subset characterized by the absence of both IgD and CD27 (double-negative, DN) in systemic lupus erythematosus (SLE) patients, thus being postulated that they could represent a novel memory population [4]. Additional heterogeneity within the DN population has been recently established, where these cells comprise four major subsets: DN1 to DN4 B cells, based on their relative expression of CD21 and CD11c [3, 5, 6]. Although not clear yet, it has been suggested that DN1 may represent early activated memory cells, whereas DN2 cells would embody primed antibody-secreting cells (ASC) precursors derived from newly activated naïve cells [7]. The absence of CD21 and CD11c defines DN3 B cells, while both markers are expressed by DN4 B cells [3], but the function and significance of these subsets, particularly in contexts different from autoimmune diseases, remain to be elucidated.

Over the last couple of years, the worldwide Coronavirus disease 2019 (COVID-19) pandemic situation has been rushed the characterization of different anti-viral immune-mediated mechanisms aimed to resolve this emergent illness. COVID-19 is caused by the severe acute respiratory syndrome coronavirus 2 (SARS-CoV-2) that may evolve asymptomatically or with mild symptoms in most patients. In contrast, others suffer from acute respiratory distress syndrome (ARDS) with a poor prognosis [8]. The severity of COVID-19 depends on the balance of host immune responses against viral stimuli. In severe cases, this response is deregulated and characterized by a hyperinflammatory status originated by high levels of cytokines and pro-inflammatory molecules, known as cytokine storm [9].

Interestingly, COVID-19 patients display alterations in different myeloid and lymphoid cells that are associated with several clinical features [10, 11]; among these leucocyte subsets, B cells remain as one of the less-studied cell types in this disease with few reports that go beyond the analysis of a total $CD19^{+}$ B cell population in small or limited cohorts of patients [6, 12]. In this context, the contribution to disease of rare B cell subsets such as DN subpopulations remains poorly understood.

According to their phenotype, DN B cells could be contained in the subset commonly referred to as atypical B cells, observed at high frequencies during autoimmune disease including arthritis or SLE, and chronic infections with hepatitis C virus, human immunodeficiency virus (HIV), or malaria [4, 13–16]. Some authors consider these B cells as anergic or exhausted due to chronic antigenic stimulation since some express high levels of inhibitory receptors, such as Fc-receptor-like (FCRL) molecules [15]. However, this population's "exhausted" description is conflicting with the previously mentioned SLE patients exhibiting high numbers of these atypical B cells, which have been proposed as activated lymphocytes in the process of differentiation to ASC [7]. Accordingly, it has been shown that their specific B cell receptors (BCRs) to *Plasmodium falciparum* could also contribute to the anti-parasitic antibodies' generation [17]. As similar B cell phenotypes arise after influenza or yellow fever vaccination, vaccinia immunization, and primary HIV infection [18, 19], it could be suggested that these cells are part of protective immune responses.

Table 1 Features of COVID-19 patients

Characteristic	Healthy individuals ($n=15$)	All patients ($n=91$)	Mild/moderate ($n=24$)	Severe ($n=35$)	Critical ($n=32$)
Gender—number (%)					
Female	6 (40)	31 (34)	10 (42)	16 (46)	5 (16)
Male	9 (60)	60 (66)	14 (58)	19 (54)	27 (84)
Age in years—median (range)	45 (24–64)	48 (23–80)	32 (25–68)	50 (23–80)	54 (33–80)
Diagnosis of SARS-COV-2 (%)					
PCR + (nasopharyngeal swab)	0 (0)	91 (100)	24 (100)	35 (100)	32 (100)
Days of symptoms—median (range)	NA	7 ± 5.1 (1–30)	3.5 ± 4.3 (1–21)	9 ± 4.7 (1–22)	8 ± 5.2 (3–30)
Measure of illness severity and vital signs—median ± SD					
NEWS	ND	8 ± 3.66	2 ± 1.56	8 ± 2.55	10 ± 2.19
Respiratory rate	ND	24 ± 9.99	18 ± 3.57	24 ± 6.95	35.5 ± 9.23
SO_2	ND	88 ± 17.18	95 ± 2.2	88 ± 9.69	62 ± 17.53
PaO_2/FiO_2	ND	244 ± 108.5	304.8 ± 11.33	247 ± 104.7	98 ± 82.2
Laboratory values—median ± SD					
White blood cell count, cells/μL	5200 ± 1189	8200 ± 4620	6200 ± 3833	7900 ± 3837	10,950 ± 5146
Lymphocyte count, cells/μL	1058 ± 516.40	925 ± 689.50	1435 ± 1023	851 ± 363.3	695 ± 441
Neutrophil count, cells/μL	ND	6100 ± 4936	3715 ± 1618	6100 ± 3768	9158 ± 5761
Neutrophil to lymphocyte ratio	ND	6.75 ± 14.28	2.29 ± 9.15	6.75 ± 7.41	12.56 ± 19.5
Albumin, g/dL	ND	3.6 ± 0.69	4.63 ± 0.36	3.74 ± 0.45	3.1 ± 0.49
Alanine aminotransferase, U/L	ND	37.5 ± 4865	25.5 ± 18.8	40 ± 7447	37.9 ± 186
Aspartate aminotransferase, U/L	ND	36.8 ± 118	23 ± 8.27	47 ± 28.36	45.8 ± 183.2
C-reactive protein, mg/dL	ND	11.4 ± 9.94	0.77 ± 3.26	9.99 ± 8.83	18.37 ± 9
Lactate dehydrogenase, U/L	ND	330.5 ± 199.7	178.5 ± 36.23	304 ± 122.8	501 ± 212.1
Fibrinogen, mg/dL	ND	611.5 ± 192.8	353 ± 110.3	611.5 ± 172.1	654 ± 161
D-dimer, ng/mL	ND	672 ± 2329	313 ± 136.6	497.5 ± 913.4	1472 ± 3224
Troponin, pg/mL	ND	5.7 ± 286.4	2.05 ± 1.21	4.2 ± 5.24	14.8 ± 433.5
Cytokines values—median ± SD					
IL-1RA, pg/mL	ND	60.2 ± 387.6	47.98 ± 36.19	57.13 ± 249.2	92.08 ± 587
IL-6, pg/mL	ND	24.19 ± 95.43	13.27 ± 69.18	21.13 ± 60.25	42.13 ± 133
IL-10, pg/mL	ND	15.3 ± 84.41	13.38 ± 25.47	14.71 ± 108.3	25.94 ± 84.17
IL-18, pg/mL	ND	632 ± 546.4	516.7 ± 215.9	555.9 ± 705.2	987.6 ± 420
MCP-1, pg/mL	ND	531.7 ± 387.3	497 ± 867.5	541.5 ± 270.6	601.3 ± 525.6
IP-10, pg/mL	ND	1621 ± 2084	1081 ± 12.02	1701 ± 2031	3194 ± 2412
Outcomes—number (%)					
Admission to hospital	0 (0)	67 (74)	0 (0)	35 (100)	32 (100)
Death	NA	18 (20)	0 (0)	4 (11)	14 (44)
Recovery	NA	73 (80)	24 (100)	31 (89)	18 (56)

SO_2 oxygen saturation, *NEWS* National Early Warning Score, *FiO_2* fraction of inspired oxygen, *PaO_2* partial pressure of oxygen, *PaO_2/FiO_2* ratio of arterial oxygen partial pressure to fractional inspired oxygen, *NA* not applicable, *ND* not determined, *SD* standard deviation

To elucidate if DN B cells could be friend or foe during SARS-CoV-2 acute infection, we analyzed the numbers of these cell compartments in peripheral blood of COVID-19 patients with different disease severity and found several differences that seem to contribute to segregate the disease severity status.

Methods

COVID-19 patients and healthy donors

91 COVID-19 patients and 15 healthy donors were recruited at Instituto Nacional de Ciencias Médicas y Nutrición Salvador Zubirán in Mexico City, Mexico. All patients confirmed by a positive PCR test for SARS-CoV-2 were invited to be included in the study. Upon admission, vital signs including

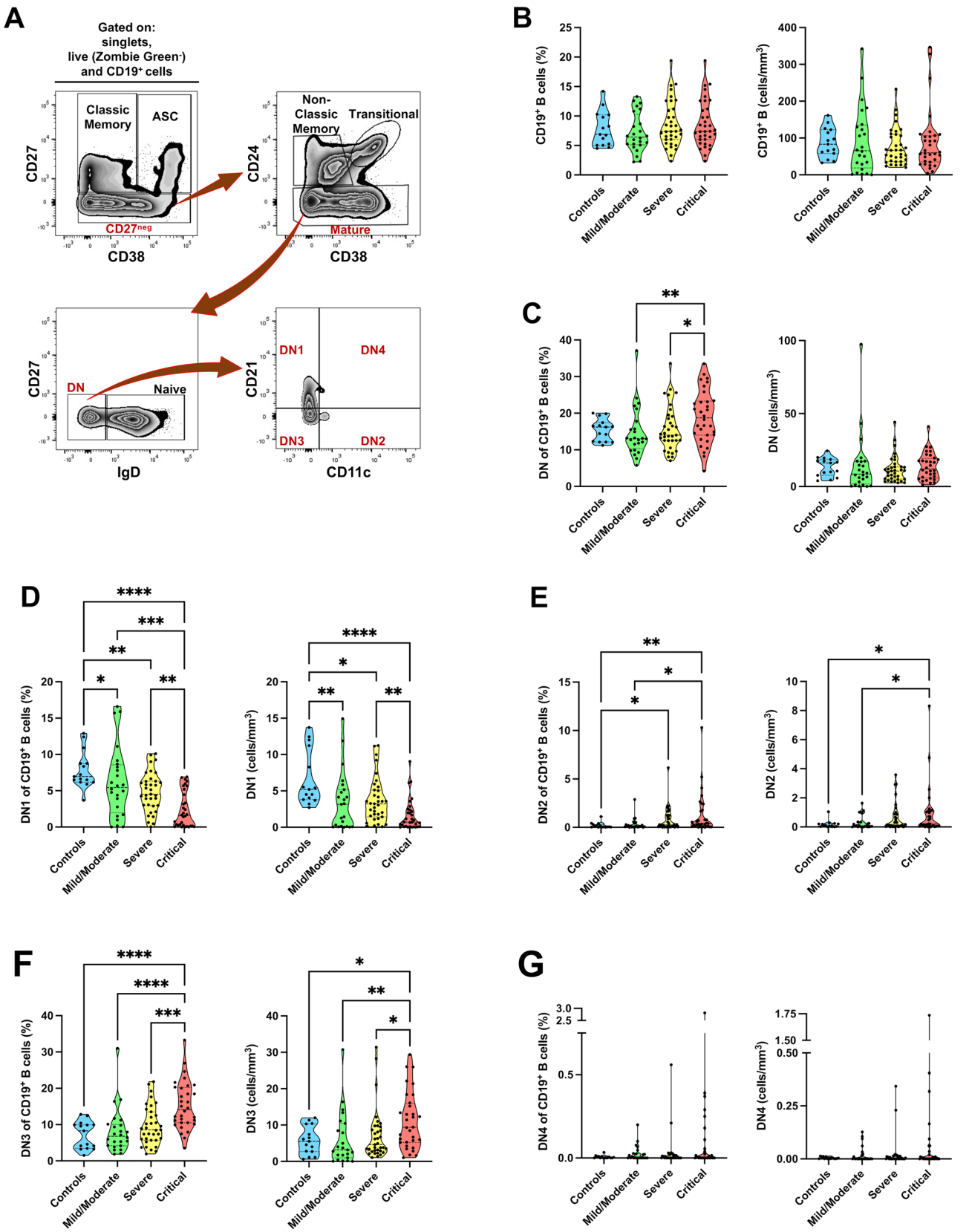
A
Gated on:
singlets,
live (Zombie Green-)
and CD19+ cells
Classic Memory
ASC
CD27
CD27neg
CD38
Non-Classic Memory
Transitional
CD24
Mature
CD38
DN
Naive
CD27
IgD
DN1
DN4
DN3
DN2
CD21
CD11c
B
CD19+ B cells (%)
CD19+ B (cells/mm3)
C
DN of CD19+ B cells (%)
DN (cells/mm3)
D
DN1 of CD19+ B cells (%)
DN1 (cells/mm3)
E
DN2 of CD19+ B cells (%)
DN2 (cells/mm3)
F
DN3 of CD19+ B cells (%)
DN3 (cells/mm3)
G
DN4 of CD19+ B cells (%)
DN4 (cells/mm3)
Controls
Mild/Moderate
Severe
Critical

◂**Fig. 1** DN B cell subsets in COVID-19 patients. **A** Gating strategy for the identification of the indicated B cell subsets in PBMCs (depicting representative results from a healthy control) previously selected from singlets gate (SSC-A vs. SSC-H), live Zombie $Green^-$ cells gate, and total $CD19^+$ B cells gate. **B** Comparative analysis of total frequencies of $CD19^+$ B cells on the left panel and absolute numbers on the right panel. **C** Comparative analysis of total DN cells; frequencies relative to $CD19^+$ B cells on the left panel and absolute numbers on the right panel. **D** Comparative analysis of DN1 subset; frequencies relative to $CD19^+$ B cells on the left panel and absolute numbers on the right panel. **E** Comparative analysis of DN2 subset. **F** Comparative analysis of DN3 subset. **G** Comparative analysis of DN4 subset. All frequency or absolute number values are displayed as mean (dashed line) plus lower and upper quartiles (dotted lines). Patients infected with SARS-CoV-2 ($n=91$), subdivided in mild/moderate ($n=24$), severe ($n=35$) or critical ($n=32$) disease groups plus healthy controls ($n=15$, negative PCR for SARS-CoV-2) were included in all graphs. The data were analyzed by a Kruskal–Wallis test followed by a Dunn's post hoc test. *$p \le 0.05$, **$p \le 0.01$, ***$p \le 0.001$, ****$p \le 0.0001$

respiratory rate (RR) and oxygen saturation (SO_2), plus the number of days after symptom onset (DaSO) information were collected. Laboratory tests were taken, including arterial blood gas analysis, leukocyte (Lk), lymphocyte (Lt), and neutrophil (Nt) counts, liver function tests (alanine aminotransferase; ALT, and aspartate aminotransferase; AST), albumin (Alb), C-reactive protein (CRP), lactate dehydrogenase (LDH), fibrinogen (Fib), D-dimer (Dd), troponin (Trp). Additionally, the National Early Warning Score (NEWS) was determined for each patient. The severity of the disease was classified in the following patient groups: mild/moderate ($n=24$): fever, signs of airway disease, with or without a tomographic image indicating pneumonia. Severe ($n=35$): any of the following: $SO_2 < 92\%$ at rest, respiratory rate > 30 rpm, respiratory failure, arterial partial pressure of oxygen (PaO_2)/fraction of inspired oxygen (FiO_2) ratio (PaO_2/FiO_2 or PaFi) < 300 mmHg. Critical ($n=32$): any of the following: requirement for mechanical ventilation, shock, or concomitant organ failure [20]. PCR test-negative individuals without respiratory symptoms were recruited as controls. Samples from reported asthmatic, HIV, cancer, autoimmune disease, or pregnant individuals (both patients and controls) were not included in this study. All the available demographic information and features of these patients and controls are depicted in Table 1.

All recruited individuals signed an informed consent prior to the inclusion. The Instituto Nacional de Ciencias Médicas y Nutrición Salvador Zubirán (Mexico) Ethics and Research Institutional Committees approved the study (Ref. 3341) in compliance with the Helsinki declaration.

Multiparametric flow cytometry analysis

Peripheral blood mononuclear cells (PBMCs) were isolated by density gradients with Ficoll-Paque (GE Healthcare Life Sciences). Recovered cells were resuspended in RPMI-1640 (Gibco) and counted before staining procedures with the following conjugated monoclonal antibodies BUV496 anti-human CD19 (BD Horizon), Brilliant Violet 650 anti-human CD38, APC/Cy7 anti-human CD27, Brilliant Violet 421 anti-human CD24, PerCP/Cyanine5.5 anti-human IgD, Alexa Fluor 700 anti-human CD21, PE/Dazzle 594 anti-human CD11c and Zombie Green dye (all from BioLegend). For staining, 2×10^6 cells were treated with human a FcX blocker (BioLegend) for 10 min, then incubated for 30 min at 4 °C with the antibody cocktail, washed, and fixed with fixation buffer (BioLegend) for 1 h. Lastly, cells were washed once with cell staining buffer (BioLegend) and then resuspended in 300 µL of the same buffer for immediate flow cytometric analysis on a BD LSRFortessa using FACSDiva software (BD Biosciences), acquiring at least 1×10^6 cells. Files were analyzed using FlowJo v10 software (BD Biosciences) with the strategy shown in Fig. 1A, using Fluorescence Minus One (FMO) controls to define gates plus CompBeads (BD Biosciences) and single stained fluorescent samples to achieve compensation.

Cytokine and chemokine determinations

The concentrations of six cytokines and chemokines: IL-1RA, IL-6, IL-10, IL-18, monocyte chemoattractant protein 1 (MCP-1)/CCL2, and interferon gamma-induced protein (IP-10)/CXCL10, in serum of the patients, were measured using the MILLIPLEX MAP Human Cytokine/Chemokine Magnetic Bead Panel kit (EMD Millipore) on a 2-laser Bio-Plex 200 suspension array system combined with a Bio-Plex Pro Wash Station (both from Bio-Rad), according to the manufacturer's instructions. Bead-fluorescence intensity readings for all the samples and standards were converted into the corresponding analyte concentrations employing the Bio-Plex Manager software v6.2 (Bio-Rad). The included cytokines and chemokines were selected among our available multiplex assays, according to the previous reports regarding their potential utility as blood-associated prognostic biomarkers in patients with COVID-19 [8, 21].

Statistics and bioinformatics analysis

Principal component analysis (PCA) method was performed on RStudio (1.3), running on R software (4.0). All

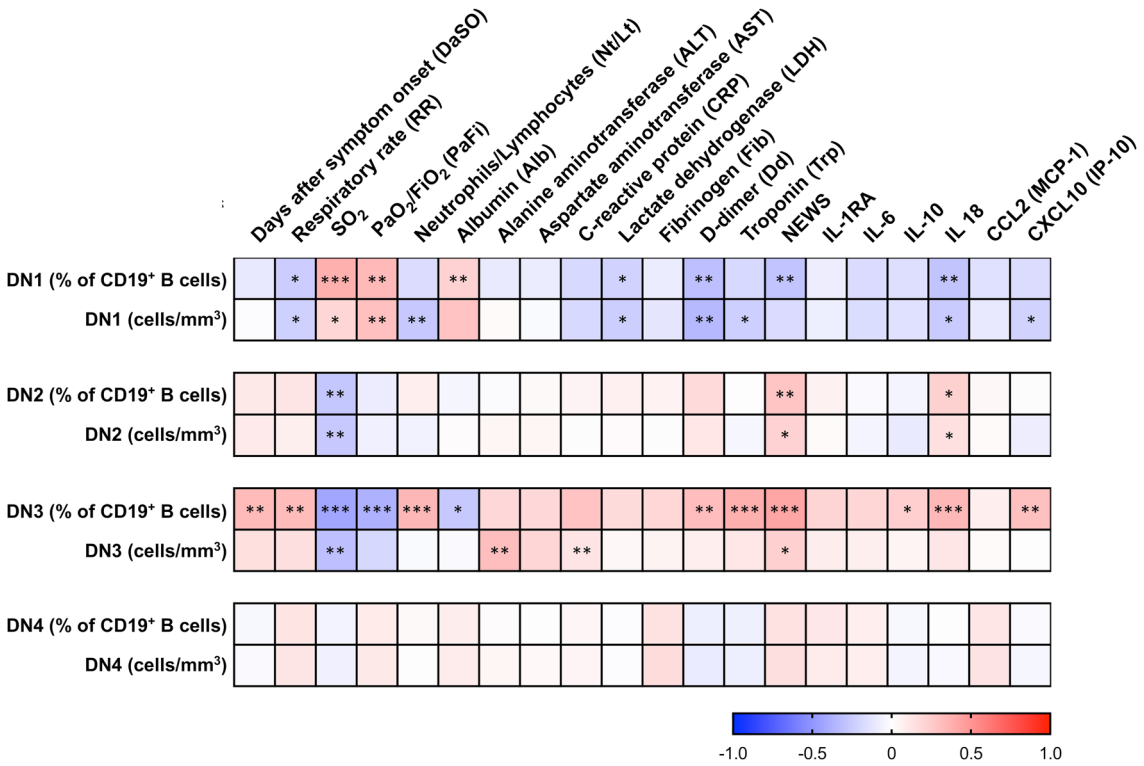

Fig. 2 DN subsets correlate with COVID-19-patient features. Correlation matrix showing a graphical representation of calculated Spearman's coefficient calculations between the B cell subset frequencies and indicated serum cytokines, clinical and laboratory variables of total COVID-19 patients ($n=91$) in our cohort. The underlying color scale indicates Spearman's coefficient values. *$p \leq 0.05$, **$p \leq 0.01$, ***$p \leq 0.001$

numerical variables were scaled to have unit variance before the analysis. PCA was processed with FactoMineR library and graphically produced with Factoextra package. We used fviz_pca_biplot() function to represent DN variables contribution and their relation to patients disease severity. We presented a bar plot of variables using fviz_pca_biplot() to visualize the three dimensions global contribution. Moreover, we employed Matlab on 20b version for plotting three-dimensional PCA representation.

Results

DN B cell subsets are altered in COVID-19 patients

To identify DN subsets in peripheral blood, we segregate $CD27^-$ cells from total $CD19^+$ B cells. We then exclude $CD24^+$ cells to select a "mature" population composed by IgD^+ naïve B cells and the remaining DN IgD^- cells, further subdivided into four subsets: DN1, DN2, DN3, and DN4, based on their CD11c and CD21 expression. This gating strategy is depicted in Fig. 1A.

When total frequency or absolute $CD19^+$ cell numbers were analyzed, we did not find significant differences in the B cell compartment between healthy subjects and COVID-19 patients of any category (Fig. 1B), as reported previously by our research group and also by other authors [12, 22]. We also found that conventional circulating B cell subsets, including transitional (T1/T2) $CD24^{hi}$ $CD38^{hi}$ $CD27^-$, naïve $CD38^{lo/-}$ $CD27^-$ IgD^+, unswitched-memory (USwM) $CD27^+$ IgD^+, switched-memory (SwM) $CD27^+$ IgD^+, and plasmablasts (ASC) $CD38^{hi}$ $CD27^{hi}$ exhibited similar trends to what has been informed in recent literature [6, 12] with the expansion of immature B cells in mild/moderate COVID-19, increase of plasmablasts in severe and critical patients, and a loss of memory subsets in almost all patients (Supplemental Fig. 1). Interestingly, some differences emerged when total DN cell frequencies were compared, particularly among mold/moderate and severe or critical patients (Fig. 1C). Outstandingly, several significant changes could be detected when each DN subset was analyzed: DN1 cell frequencies and absolute numbers from COVID-19 patients appeared as decreased when compared with healthy donors, a feature that seems to be more pronounced according to the disease severity (Fig. 1D). In contrast, DN2 cells exhibited a slight increase, most noticeable when critical patients were analyzed (Fig. 1E). Similarly, significant increments in the DN3 cell frequencies and absolute numbers in the

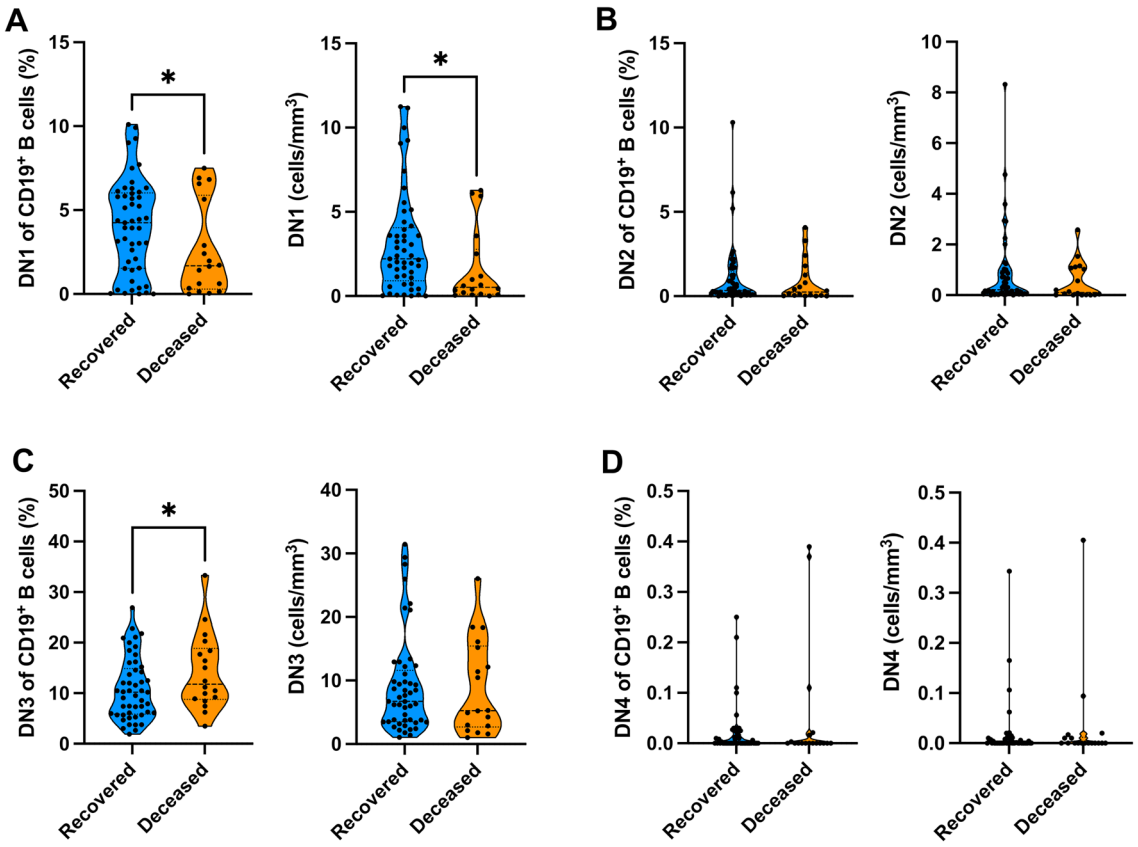

Fig. 3 Numbers of DN B cell subsets according to COVID-19 hospitalized patients' outcome. Comparative analysis of DN1 (**A**), DN2 (**B**), DN3 (**C**), or DN4 (**D**) frequencies relative to $CD19^+$ B cells and absolute numbers according to severe and critical (hospitalized) COVID-19 patients' ($n=67$) outcomes. The data were analyzed by a Kruskal–Wallis test followed by a Dunn's post hoc test. * $p \leq 0.05$

patients were also detected (Fig. 1F) but appearing much more robust than the DN2 counterparts. Finally, the DN4 fraction was seen almost absent from circulation in all the groups analyzed, finding no significant differences in their numbers (Fig. 1G).

DN subpopulations are associated with different clinical "signatures" of COVID-19

To elucidate the potential roles of these rare B cell subsets, we tried to associate their amounts in peripheral blood to the patients' available clinical and laboratory features, presented in Table 1 and compared among COVID-19 groups in Supplemental Fig. 2. When correlation analyses including all variables were performed, it becomes evident that each DN subset displayed a specific matrix pattern (Fig. 2). Interestingly, the DN1 frequencies and absolute numbers patterns stand out since they revealed mainly negative (several significant) correlations with many of the analyzed parameters, mainly related to a pro-inflammatory status in COVID-19 patients [23, 24]. Correspondingly, DN1 numbers positively correlated with oxygen parameters (SO_2 and PaFi) and show a negative correlation with a surrogate of inflammation, such as albumin. Contrastingly, the remaining DN subsets exhibited opposite patterns, a feature that is particularly marked when the DN3 cell frequencies or absolute numbers are seen.

Additionally, when the outcomes of severe and critical (hospitalized) patients were analyzed, we observed exciting differences: DN1 cells were detected as significantly reduced in their frequency and absolute numbers in deceased individuals when compared to recovered ones (Fig. 3A); contrariwise, the DN3 subset appeared slightly increased in the deceased patients, with a significant difference only when frequencies were analyzed (Fig. 3C). Finally, no outcome differences were observed when DN2 or DN4 cell numbers were examined (Fig. 3B, D).

DN B cell subset segregate critical and mild/moderate COVID-19 patients

We segregate COVID-19 patients by analyzing all available clinical and laboratory variables plus DN1, DN2, and DN3 subsets frequencies and absolute numbers (DN4 values were

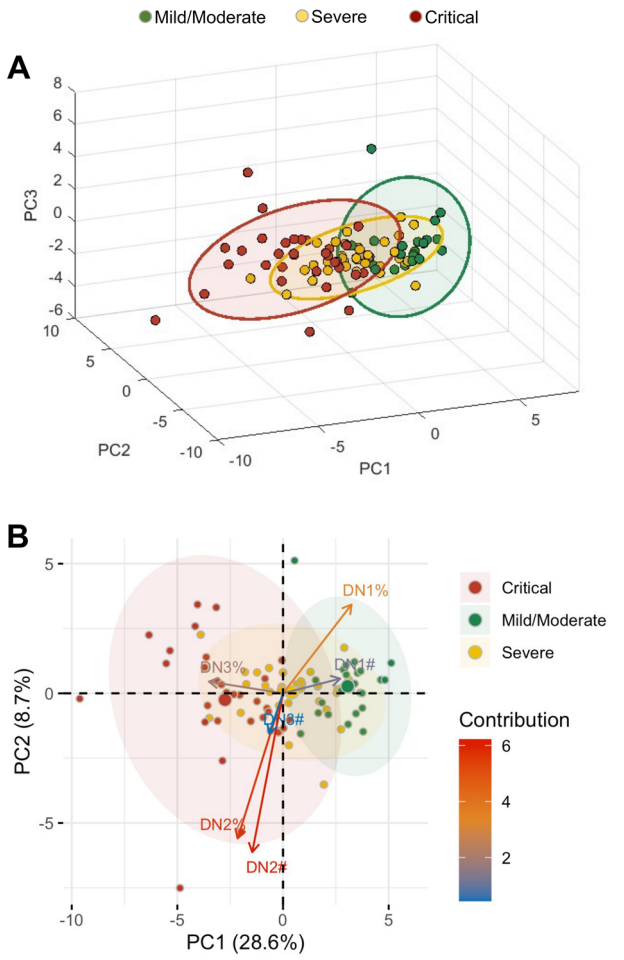

Fig. 4 DN B cells contribute to segregate COVID-19 patients by severity of the disease. 3-D (**A**) and 2-D (**B**) views of PCA considering all measured variables in COVID-19 patients, including the frequencies (%) and absolute numbers (#) of DN1, DN2, and DN3 subsets, clinical/laboratory values (respiratory rate, oxygen saturation, arterial partial pressure of oxygen/fraction of inspired oxygen ratio, days after symptom onset, leukocyte, lymphocyte, and neutrophil counts, alanine aminotransferase, aspartate aminotransferase, albumin, C-reactive protein, lactate dehydrogenase, fibrinogen, D-dimer, troponin, and National Early Warning Score) and cytokines (IL-1RA, IL-6, IL-10, IL-18, MCP-1, and IP-10). Each point represents a single patient projected to the first principal components, and colors are associated with the COVID-19 severity, as indicated. The 2-D view includes arrows representing the relative contributions of each of DN cell subsets, according to the indicated scale. The 3-D view only includes patients' projection and severity but including three principal components. Both views contain 95% confidence ellipses

excluded since these cells were almost absent in patients and did not contribute to groups segregation), using PCA in a 3D scatter-plot visualization (Fig. 4A). Axes include the three components with a higher proportion of the variation, 28.6%, 8.7%, and 6.4%, respectively. The plotted data represent 43.7% of the complete data variation, making it more informative and accurate for interpretation. Also, we have included 95% confidence ellipses to show intersection areas among severity.

We also deliver a 2D scatter-biplot to visualize our DN B cells' influential degree independently between principal components 1 and 2 (Fig. 4B). We observed that the group of variables: DN2 frequency (where frequency is denoted as %), DN2 absolute counts (where absolute counts are symbolized as #), and DN3#, are positively correlated. A negative correlation among DN1% and the latter group of variables can be observed, and in the same way between DN1# and DN3%. The most explainable variables are determined by vectors magnitude (arrows size) being DN1%, DN2%, and DN2#. Finally, the fact that the presence of DN1 subset is correlated with mild/moderate patients is validated as well as for DN2/3 subsets with critical patients.

Discussion

Although B cells' contribution to infection resolution is usually set at advanced or chronic stages, there are some reports suggesting that some subsets of this lineage could participate during acute phases of infectious disease, in other ways different from antibody secretion. Such "atypical" B lymphocytes, which certainly possess innate-like properties due to their high Toll-like receptors (TLRs) responsiveness, include the DN cells that are notably expanded in viral or parasitic infections, as well as autoimmune disorders [3, 25, 26].

Apart from the DN2 subset, that has been previously reported as expanded in SLE, Hepatitis C or HIV infection [3, 27], more recently in COVID-19 [12], and described as primed plasma cell precursors differentiated through an extra-follicular pathway [7]; almost nothing is known about the remaining DN subpopulations. Interestingly, we found significant alterations in DN1, DN2, and DN3 subsets during COVID-19 acute development in this work.

As expected, the DN2 subset was found expanded in COVID-19, increasing according to the disease severity but predominantly on the critical patients. That change could be explained by the prominent proinflammatory environment raised by these individuals; in our cohort, this could be evidenced by the positive correlation of these DN2 cells with IL-18 amounts, which could probably be involved in their expansion since it is associated with type 1 immune responses [28] that seem to be necessary for their

differentiation [29]. As DN2 also demonstrated positive correlations with disease severity indicators (such as SO_2 or NEWS), the notion of a contributing proinflammatory milieu is again supported. However, we cannot discard these cells' direct influence on disease aggravation since their proinflammatory profile has been described previously [30, 31].

Like DN2, the DN3 subset displayed a similar but ever more robust expansion, enhanced in more severe patients; interestingly, this feature is more strongly associated with an inflammatory-associated pattern, where inflammation markers positively correlate with DN3 amounts whereas ventilatory parameters show the opposite. Additionally, DN3 augmented proportion appears to be linked to worse outcomes in more severe patients, making us suspect a proinflammatory function of these cells. Despite having a complete unknown function or origin, COVID-19 seems is the only reported condition where DN3 cells are overrepresented, positioning them as exciting candidates for further studies.

On the other hand, DN1 cells exhibited a reduction in their amounts in COVID-19, being more evident in critical cases. When correlation analyses with clinical/laboratory features and cytokines were done, DN1 cell numbers displayed an opposite pattern than DN2 or DN3 cells, where several negative correlations with proinflammatory elements plus positive values for ventilatory parameters were observed. Hence, the high number of DN1 cells seems to be associated with a less severe disease course and even a better outcome in hospitalized patients. Again, since nothing is reported about this subset's functional roles, we can only argue about their anti-inflammatory potential since it has been reported that cells with a similar phenotype to DNs have been documented to enhance $CD4^+CD25^{hi}$ regulatory T cells (Treg) proliferation in vitro [32]. In this way, it is possible that the DN1 subgroup could contain a non-previously described regulatory B cells (Breg) population, helping to maintain homeostasis in mild/moderate COVID-19 but being lost in severe or critical cases.

Finally, as we employ the DN subset amounts together with some clinical/laboratory descriptors and cytokines (previously described as relevant as prognostic biomarkers in COVID-19 [8, 21]) for multivariate approaches, we conclude that the measurement of these cells can definitively support the segregation of patients according to disease severity, where mild/moderate and severe/critical patients exhibit major segregating-contributions of DN1 and DN2/DN3, respectively, with similar or even better robustness than most of the variables studied here (Supplemental Fig. 3). The usefulness of these DN subset measurements as potential biomarkers for prognostic approaches is a feature that is not possible to determine in our cohort and needs to be addressed by a longitudinal study that possibly will shed light regarding the pathogenic or protective functional roles of these traditionally neglected B cells.

Supplementary Information The online version contains supplementary material available at https://doi.org/10.1007/s00011-021-01525-3.

Acknowledgements Rodrigo Cervantes-Díaz is a doctoral student from the Programa de Doctorado en Ciencias Biomédicas, Universidad Nacional Autónoma de México (UNAM) and has received the Consejo Nacional de Ciencia y Tecnología (CONACyT) fellowship 736793/CVU 821078. Víctor Andrés Sosa-Hernández has received the Consejo Nacional de Ciencia y Tecnología (CONACyT) fellowship 484600. Miriam Pescador-Rojas acknowledges support from IPN project SIP 20211942. Our study received assistance from the Flow Cytometry Unit at the Red de Apoyo a la Investigación/Instituto Nacional de Ciencias Médicas y Nutrición.

Author contributions RC-D and VAS-H contributed equally to the design and performance of experiments, analysis, and interpretation of data. RC-D, VAS-H, JJT-R, and SR-R performed experiments and analyzed data. MC-H, JCP-F and DEM-S assisted in processing and preservation of control and patient samples. AP-F collected patient data, generated, and organized our clinical database. RC-D, VAS-H, and DG-M participate in writing and editing the manuscript. MP-R and VAS-H performed bioinformatics and statistical analyses. JLM-M designed and performed experiments, supervised general work, wrote, and edited the manuscript. All authors contributed to the article and approved the submitted version.

Funding This work was supported by CONACyT [Grants A3-S-36875, F0005-2020–01-313252] and UNAM-DGAPA-PAPIIT Program [Grants IN213020, IN212122].

Data availability The data that support the findings of this study are available from the corresponding author, upon reasonable request.

Declarations

Conflict of interest The authors declare that the research was conducted in the absence of any commercial or financial relationships that could be construed as a potential conflict of interest.

Ethical approval All recruited individuals signed an informed consent prior to the inclusion. The Instituto Nacional de Ciencias Médicas y Nutrición Salvador Zubirán (Mexico City, Mexico) ethics and research committees approved the study (Ref. 3341) in compliance with the Helsinki declaration.

References

1. Perez-Andres M, Paiva B, Nieto WG, Caraux A, Schmitz A, Almeida J, et al. Human peripheral blood B-cell compartments: a crossroad in B-cell traffic. Cytometry B Clin Cytom. 2010;78(Suppl 1):S47-60.
2. Glass DR, Tsai AG, Oliveria JP, Hartmann FJ, Kimmey SC, Calderon AA, et al. An integrated multi-omic single-cell atlas of human B cell identity. Immunity. 2020;53:217–32.
3. Sanz I, Wei C, Jenks SA, Cashman KS, Tipton C, Woodruff MC, et al. Challenges and opportunities for consistent classification of human B cell and plasma cell populations. Front Immunol. 2019;10:2458.

4. Wei C, Anolik J, Cappione A, Zheng B, Pugh-Bernard A, Brooks J, et al. A new population of cells lacking expression of CD27 represents a notable component of the B cell memory compartment in systemic lupus erythematosus. J Immunol. 2007;178:6624–33.
5. Stewart A, Ng JC, Wallis G, Tsioligka V, Fraternali F, Dunn-Walters DK. Single-cell transcriptomic analyses define distinct peripheral B cell subsets and discrete development pathways. Front Immunol. 2021;12:602539.
6. Woodruff MC, Ramonell RP, Nguyen DC, Cashman KS, Saini AS, Haddad NS, et al. Extrafollicular B cell responses correlate with neutralizing antibodies and morbidity in COVID-19. Nat Immunol. 2020;21:1506–16.
7. Jenks SA, Cashman KS, Zumaquero E, Marigorta UM, Patel AV, Wang X, et al. Distinct effector B cells induced by unregulated toll-like receptor 7 contribute to pathogenic responses in systemic lupus erythematosus. Immunity. 2018;49:725–39.
8. Schultze JL, Aschenbrenner AC. COVID-19 and the human innate immune system. Cell. 2021;184:1671–92.
9. Mangalmurti N, Hunter CA. Cytokine storms: understanding COVID-19. Immunity. 2020;53:19–25.
10. Kvedaraite E, Hertwig L, Sinha I, Ponzetta A, Hed Myrberg I, Lourda M, et al. Major alterations in the mononuclear phagocyte landscape associated with COVID-19 severity. Proc Natl Acad Sci USA. 2021;118(6):2018587118.
11. Rupp J, Dreo B, Gutl K, Fessler J, Moser A, Haditsch B, et al. T Cell phenotyping in individuals hospitalized with COVID-19. J Immunol. 2021;206:1478–82.
12. Sosa-Hernandez VA, Torres-Ruiz J, Cervantes-Diaz R, Romero-Ramirez S, Paez-Franco JC, Meza-Sanchez DE, et al. B cell subsets as severity-associated signatures in COVID-19 patients. Front Immunol. 2020;11:611004.
13. Isnardi I, Ng YS, Menard L, Meyers G, Saadoun D, Srdanovic I, et al. Complement receptor 2/CD21- human naive B cells contain mostly autoreactive unresponsive clones. Blood. 2010;115:5026–36.
14. Charles ED, Brunetti C, Marukian S, Ritola KD, Talal AH, Marks K, et al. Clonal B cells in patients with hepatitis C virus-associated mixed cryoglobulinemia contain an expanded anergic CD21low B-cell subset. Blood. 2011;117:5425–37.
15. Moir S, Ho J, Malaspina A, Wang W, DiPoto AC, O'Shea MA, et al. Evidence for HIV-associated B cell exhaustion in a dysfunctional memory B cell compartment in HIV-infected viremic individuals. J Exp Med. 2008;205:1797–805.
16. Weiss GE, Crompton PD, Li S, Walsh LA, Moir S, Traore B, et al. Atypical memory B cells are greatly expanded in individuals living in a malaria-endemic area. J Immunol. 2009;183:2176–82.
17. Muellenbeck MF, Ueberheide B, Amulic B, Epp A, Fenyo D, Busse CE, et al. Atypical and classical memory B cells produce Plasmodium falciparum neutralizing antibodies. J Exp Med. 2013;210:389–99.
18. Andrews SF, Chambers MJ, Schramm CA, Plyler J, Raab JE, Kanekiyo M, et al. Activation dynamics and immunoglobulin evolution of pre-existing and newly generated human memory B cell responses to influenza hemagglutinin. Immunity. 2019;51:398–410.
19. Knox JJ, Buggert M, Kardava L, Seaton KE, Eller MA, Canaday DH, et al. T-bet+ B cells are induced by human viral infections and dominate the HIV gp140 response. JCI Insight. 2017;2(8):92943.
20. Liu W, Tao ZW, Wang L, Yuan ML, Liu K, Zhou L, et al. Analysis of factors associated with disease outcomes in hospitalized patients with 2019 novel coronavirus disease. Chin Med J (Engl). 2020;133:1032–8.
21. Vabret N, Britton GJ, Gruber C, Hegde S, Kim J, Kuksin M, et al. Immunology of COVID-19: current state of the science. Immunity. 2020;52:910–41.
22. Lucas C, Wong P, Klein J, Castro TBR, Silva J, Sundaram M, et al. Longitudinal analyses reveal immunological misfiring in severe COVID-19. Nature. 2020;584:463–9.
23. Huang W, Li M, Luo G, Wu X, Su B, Zhao L, et al. The inflammatory factors associated with disease severity to predict COVID-19 progression. J Immunol. 2021;206:1597–608.
24. Olbei M, Hautefort I, Modos D, Treveil A, Poletti M, Gul L, et al. SARS-CoV-2 causes a different cytokine response compared to other cytokine storm-causing respiratory viruses in severely ill patients. Front Immunol. 2021;12:629193.
25. Sutton HJ, Aye R, Idris AH, Vistein R, Nduati E, Kai O, et al. Atypical B cells are part of an alternative lineage of B cells that participates in responses to vaccination and infection in humans. Cell Rep 2021; 34:108684.
26. Romero-Ramirez S, Navarro-Hernandez IC, Cervantes-Diaz R, Sosa-Hernandez VA, Acevedo-Ochoa E, Kleinberg-Bild A, et al. Innate-like B cell subsets during immune responses: beyond antibody production. J Leukoc Biol. 2019;105:843–56.
27. Chang LY, Li Y, Kaplan DE. Hepatitis C viraemia reversibly maintains subset of antigen-specific T-bet+ tissue-like memory B cells. J Viral Hepat. 2017;24:389–96.
28. Akira S. The role of IL-18 in innate immunity. Curr Opin Immunol. 2000;12:59–63.
29. Zumaquero E, Stone SL, Scharer CD, Jenks SA, Nellore A, Mousseau B, et al. IFNgamma induces epigenetic programming of human T-bet(hi) B cells and promotes TLR7/8 and IL-21 induced differentiation. Elife. 2019;8:41641.
30. Naradikian MS, Hao Y, Cancro MP. Age-associated B cells: key mediators of both protective and autoreactive humoral responses. Immunol Rev. 2016;269:118–29.
31. Wang S, Wang J, Kumar V, Karnell JL, Naiman B, Gross PS, et al. IL-21 drives expansion and plasma cell differentiation of autoreactive CD11c(hi)T-bet(+) B cells in SLE. Nat Commun. 2018;9:1758.
32. Ray A, Khalil MI, Pulakanti KL, Burns RT, Gurski CJ, Basu S, et al. Mature IgD(low/-) B cells maintain tolerance by promoting regulatory T cell homeostasis. Nat Commun. 2019;10:190.